

Linking Reaction Kinetics of Star Shaped Polystyrene by Temperature Gradient Interaction Chromatography

Hee Cheong Lee, Wonmok Lee, and Taihyun Chang*

Department of Chemistry, Pohang University of Science and Technology, Pohang, 790-784, Korea

Jin San Yoon

Department of Polymer Science and Engineering, Inha University, Incheon, 402-751, Korea

Donna J. Frater and Jimmy W. Mays*

Department of Chemistry, University of Alabama at Birmingham, Birmingham, Alabama 35294

Received December 2, 1997; Revised Manuscript Received April 6, 1998

ABSTRACT: The linking reaction kinetics of a chlorosilane-linked polystyrene six-arm star was investigated by temperature gradient interaction chromatography using a light scattering detector. The precursor arm material ($M_w = 83\,000$) was made by anionic polymerization and end capped with isoprene, and 1,2-bis(trichlorosilyl)ethane was used as the linking agent. All the reaction intermediates, from unlinked arm to six-arm star, were successfully resolved from the aliquots taken from the reactor at various linking reaction times. From the time-varying relative abundance of the star molecules with different numbers of arms, linking reaction rate constants were determined. It was found that the linking reaction rate becomes progressively slower as the number of attached arms increases. We were able to extract the quantitative ratio of the linking rate constants, $k_5/k_4 = 0.097$ and $k_6/k_5 = 0.30$, where k_i stands for the rate constant of the reaction incorporating the i th arm to an $(i - 1)$ -arm star to form an i arm star. The larger value of k_6/k_5 than k_5/k_4 can be interpreted from the molecular structures of the linking agent and polymeric anions.

Introduction

Branched polymers are materials of rapidly growing importance in the polymer industry, and the characterization of the structure of branched polymers has been one of the major concerns in the field.^{1–7} For the rigorous characterization of a polymeric material, the relationships between dilute solution properties of the polymers and their structures need to be understood, which in turn requires the study of polymers with totally controlled architecture and narrow molecular weight distribution.^{1–13} Therefore much attention has been given to the synthesis of well-defined branched polymers. An ideal model for branched polymers is a star-shaped polymer synthesized by anionic polymerization.^{11,14,15} Various types of star polymers have been synthesized by different methods.^{11,16} The most popular method, termed the linking method, involves living polymeric monoanions made by anionic polymerization method as arms and multifunctional compounds as linking agents. Since the first example of such a preparation of star polymer by Morton et al. in 1962, well-defined star polymers of high uniformity with as many as 128 arms have been produced.^{11,14} Despite such advances in the synthesis of the star-shaped polymers, however, the understanding of the linking process has been insufficient. In the early works of Gervasi and Gosnell¹⁷ and Roovers and Bywater,¹⁸ the living anion concentration was monitored spectroscopically during the linking process to determine the amount of the living ends that had reacted; however, it could not be ascertained how many arms each star had at any one time during the linking process.

Recently Frater et al. studied the linking reaction kinetics of living polystyrenic arms to bis(trichlorosilyl)-

ethane employing a size exclusion chromatography (SEC) analysis with on-line viscometry, light scattering, and refractive index detectors.¹⁵ They measured the molecular weights, radii of gyration, and intrinsic viscosities for star components in aliquots taken from the reactor at various linking reaction times. They found that there were three distinct steps in the formation of star PS, which indicated the well-separated reaction rate constants of incorporating an additional arm. The formation of four-arm star was so fast that the reaction was practically completed within 30 min. The linking reaction toward the higher number of arms was much slower. Attachment of the fifth arm required about a week and it took over 4 weeks before the complete incorporation of the sixth arm occurred. Despite their improved description of the linking reaction kinetics, their interpretation had to rely on the average number of arms in a star polymer attached during the linking reaction process due to the limited resolution of SEC.¹⁵ Since the resolution of SEC was not high enough to separate all the star species having different number of arms, only the evolution of the average molecular weight of star polymers (i.e., the average number of arms) vs reaction time could be monitored. The variation of the hydrodynamic volume of star polymers with the increasing number of arms is not as large as linear polymers of equivalent molecular weight. Thus SEC, which separates polymer chains in terms of their hydrodynamic volume in a dilute solution, is not sensitive enough to resolve four-, five-, and six-arm star polymers.

Recently, we reported a successful application of temperature gradient interaction chromatography (TGIC) for the characterization of linear and branched PS.^{7,20–25} The resolving power of TGIC is far superior to that of

SEC. In addition, TGIC was found to be less sensitive to the molecular architecture than SEC so that it could resolve each species of the linking reaction products, i.e., one- to six-arm star PS.⁷ Exploiting the high resolution of TGIC for branched polymers, in this study we reinvestigated the linking reaction kinetics of star PS by TGIC analysis.

Experiment

The experimental details of TGIC were described in the previous report.^{7,20,21} A typical isocratic HPLC apparatus equipped with a C18 bonded silica column (Alltech, Nucleosil, 100 Å pore, 250 mm × 2.1 mm, 5 μm particle size) was used. The mobile phase was a mixture of CH₂Cl₂ and CH₃CN premixed in the ratio of 57/43 (v/v). The latter solvents were used as received from Allergic (HPLC grade). The star PS was prepared by linking living PS chains with 1,2-bis(trichlorosilyl)ethane as described previously.¹⁵ A stoichiometry, Li/Cl, of 2/1 was maintained in this reaction. Prior to the linking reaction about five units of isoprene were incorporated onto each living PS chain to reduce steric hindrance during the linking reaction. Ten star PS samples from aliquots taken from the reactor at various linking reaction times were examined. Star PS solutions were made in the same solvent as the mobile phase at a concentration of 2 mg/mL and injected through a 7125 Rheodyne injector equipped with a 20 μL sample loop. The flow rate was 0.1 mL/min. Chromatograms were recorded by a UV/vis detector (LDC Analytical, Spectrophotometer 3200) at the wavelength of 260 nm and a low-angle laser light scattering detector (LALLS, LDC Analytical, KMX 6).

For SEC analysis, the same HPLC instrument as in TGIC was used except for the following: 4 SEC columns (Polymer Lab, 2 × Mixed C, 1 × Mixed D, 1 × Mixed E) were used and the column temperature was maintained at 40 °C. Tetrahydrofuran (THF) was used as the eluent and the flow rate was 1.0 mL/min. Each sample of star PS was made in THF at a concentration of about 0.5 mg/mL and injected through a 7125 Rheodyne injector with 100 μL sample loop.

Molecular weights of a separated peak were calculated by two different methods: (1) the conventional calibration method relative to linear PS standards (M_{CAL}) and (2) light scattering analysis (M_{LS}). In the light scattering analysis, it was necessary to correct M_{LS} for the preferential sorption effect in the mixed solvent system.²⁵ Both molecular weight calculation methods are well established, and detailed procedures were previously reported.^{7,26–27}

Results and Discussion

SEC Chromatogram of Star PS. In Figure 1, the SEC chromatograms of 10 star PS's are displayed. The numbers on the plot are the linking reaction times allowed prior to termination. For easy comparison, the intensity is normalized by the total elution peak area. Star PS and unlinked arms are well separated down to the baseline. The peak appearing at around 22 mL of retention volume (V_R) is the excess arm polymer whose molecular weight is about 83 000. As listed in the first column of Table 1, $\langle M_{CAL} \rangle$ and $\langle M_{LS} \rangle$ of the unlinked arms are in good agreement each other and remain constant independent of linking reaction time. The angular bracket stands for the weight average quantity of the elution peak. The small peak appearing near 21 mL of V_R corresponds to star PS with two arms (PS₂) whose $\langle M_{CAL} \rangle$ is 170 000, close to twice as high as $\langle M_{CAL} \rangle$ of unlinked arms. It was difficult to get a precise $\langle M_{LS} \rangle$ of the two-arm species due to the low intensity of the peak; however, it was confirmed that M_{LS} of the peak corresponds to that of the two-arm species within error limit. This small PS₂ peak exists for all the samples, which may indicate a minor coupling reaction between

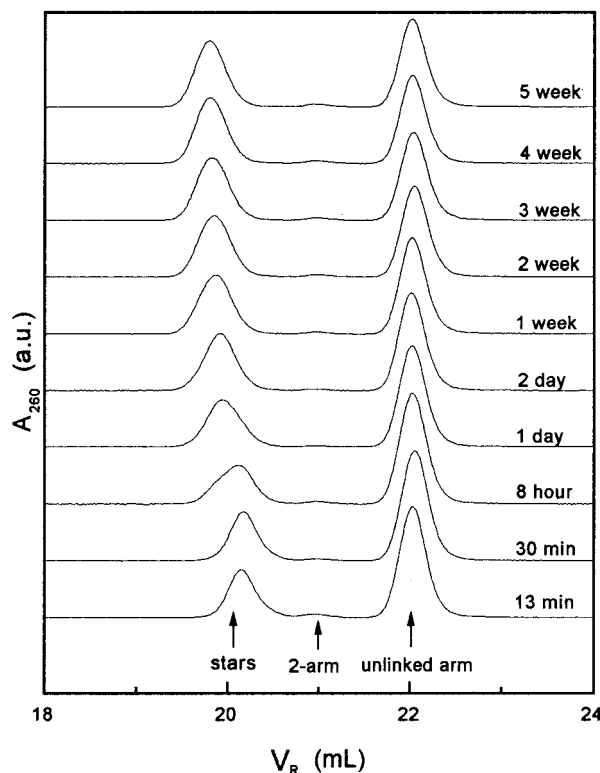


Figure 1. SEC chromatograms of 10 PS star samples taken from the reactor at the various linking reaction time which is displayed in the plot. Excess unlinked arms ($V_R = 22$ mL) and a small amount of two-arm species ($V_R = 21$ mL) are well separated, but star species having more than three-arms are eluted unresolved at $V_R = 20$ mL.

Table 1. Molecular Weights ($\times 10^3$) of Star Polymers^a

reaction time	TGIC					
	SEC $\langle M_{LS} \rangle / \langle M_{CAL} \rangle$		$\langle M_{LS} \rangle$	M_{LS} / M_{CAL}		
	arm	star		4	5	6
13 min	84.4/85.0	322/293	81.1	325/324		
30 min	83.1/84.3	322/294	81.1	322/326		
8 h	83.3/85.7	358/317	85.0	313/329	397/396	
24 h	83.0/85.7	393/343	83.1	313/333	394/388	
48 h	82.8/86.3	420/354	83.4		403/389	468/441
1 week	83.8/85.7	440/367	84.7		399/401	472/449
2 week	83.3/84.6	454/368	83.6			487/438
3 week	83.7/84.9	456/373	85.8			483/436
4 week	85.2/85.6	467/378	85.7			487/440
5 week	82.5/85.7	469/380	85.3			490/438

^a Key: M_{CAL} , molecular weight obtained from calibration with linear PS standard; M_{LS} , molecular weight obtained from on-line light scattering; $\langle \rangle$, weight average quantity.

living arms during the workup process. However, the amount is nearly negligible and is not likely involved in the linking reaction process. Therefore, it is not considered in the analysis of the linking reaction kinetics.

Star PS's of three or more arms (PS₃, PS₄, PS₅ and PS₆) appear together (single peak) near a V_R of 20 mL. They are not resolved at all, although the V_R of the peak steadily decreases as a longer reaction time is allowed, which indicates a progressive increase of the average molecular size. As listed in the second column of Table 1, both $\langle M_{LS} \rangle$ and $\langle M_{CAL} \rangle$ of the peak increase with increased linking reaction time. However, $\langle M_{LS} \rangle$ and $\langle M_{CAL} \rangle$ are no longer identical, and the deviation between the two becomes larger and larger as the reaction time increases. As elaborated in the Introduction, this

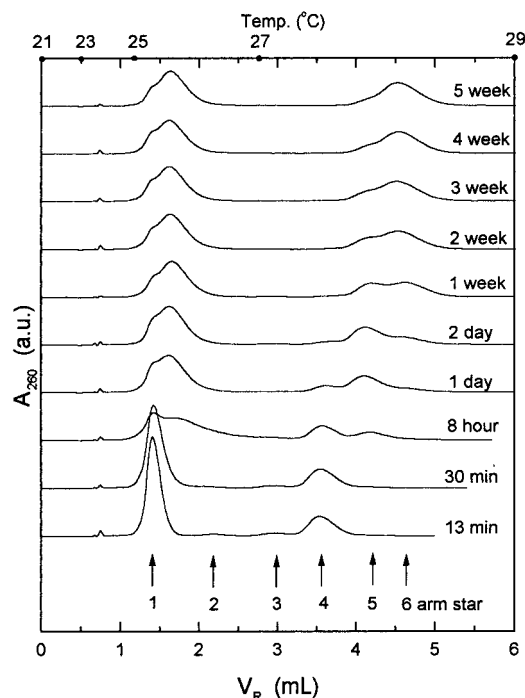


Figure 2. TGIC chromatograms of the same samples shown in Figure 1. All the species, from unlinked arm to the six-arm star, can be identified. The elution peak of unlinked arm becomes partially split and broader for the samples taken at the long reaction time. Refer to the text for the details.

is an expected behavior of SEC, which only separates the polymer chains in terms of their hydrodynamic volume.^{7,28} Since the hydrodynamic volume of the star polymer is smaller than that for the linear polymer of equivalent molecular weight, M_{CAL} is smaller than M_{LS} .⁷ The light scattering analysis is supposed to provide a true weight average molecular weight, and a $\langle M_{\text{LS}} \rangle$ of 320 000 indicates that PS_4 dominates in the early stage of the linking reaction. $\langle M_{\text{LS}} \rangle$ finally reaches the weight average molecular weight of the six-arm star, about 470 000 after the reaction for a few weeks while $\langle M_{\text{CAL}} \rangle$ reaches an asymptotic value at 380 000. This result is in good qualitative agreement with the results of Frater et al.¹⁵

TGIC chromatogram of Star PS. In Figure 2 the TGIC chromatograms of the same set of star PS as of the SEC chromatograms shown in Figure 1 are displayed. The temperature is programmed to change in four segments of linear ramp between 21 and 29 °C as shown in the upper abscissa of the plot. Injection solvent peak appears at $V_R \approx 0.8$ mL. It is evident that TGIC provides far better resolution than SEC. The chromatogram of the polymer mixture obtained after 13 min linking reaction time clearly shows four resolved peaks at $V_R = 1.4$ mL (one arm), 2.2 mL (two arm), 2.9 mL (three arm) and 3.6 mL (four arm). Five- and six-arm star molecules have yet to show up clearly at this short reaction time. Five-arm stars become clearly visible at $V_R = 4.2$ mL in the chromatogram of 8 h linking reaction time, while six-arm stars become clear only after the reaction for a few days at $V_R = 4.7$ mL. Interestingly enough, the peak of the unlinked arms starts to split, and a new broad peak appears at larger V_R . The peak splitting and broadening is clearly displayed at V_R around 1.7 mL in most of the chromatograms except for two at the early stage of linking reaction. This peculiar behavior is not observed in the

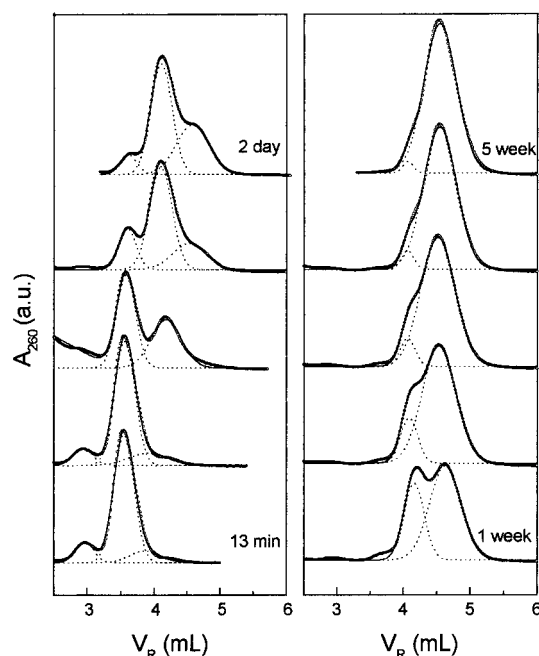


Figure 3. Separation of overlapped peaks of PS_3 , PS_4 , PS_5 , and PS_6 assuming Gaussian peak shape: open circles, experimental chromatogram; dotted line, separated Gaussian peak; solid line, sum of separated Gaussian peaks.

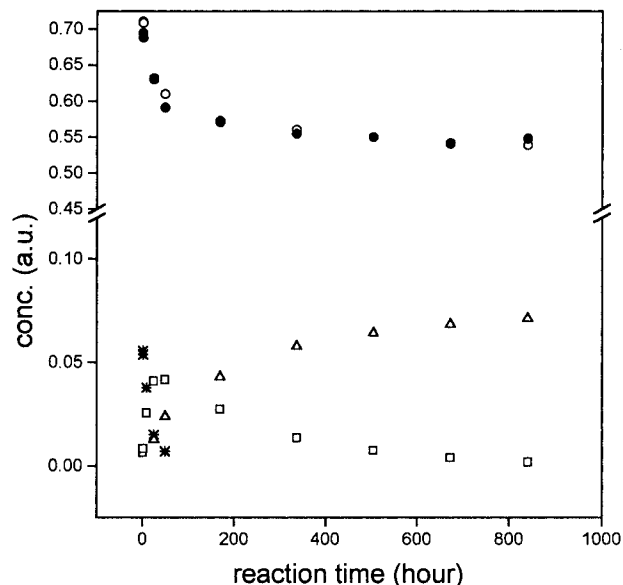


Figure 4. Relative population of each species normalized by the initial number of living arms: (○) unlinked arm (by TGIC); (●) unlinked arm (by SEC); (*) four-arm star; (□) five-arm star; (△) six-arm star.

SEC analysis. As shown in the equivalent SEC chromatograms in Figure 1, the V_R and the peak width of the elution peak of the unlinked arm species remain practically unchanged during the whole reaction period. In addition, the relative integrated areas of the unlinked arms in SEC (unimodal peak at $V_R = 22$ mL) and in TGIC (the broad bimodal peak at $1.2 \text{ mL} < V_R < 2.5 \text{ mL}$) are identical as elaborated later. (Figure 4). Furthermore, as shown in Table 1, the $\langle M_{\text{LS}} \rangle$ does not change significantly with peak broadening. A small difference between the normal (81 000) and broadened peak (85 000) appears to come from the contribution of two-arm species since the broadened peak overlaps with the PS_2 peak. Also $\langle M_{\text{LS}} \rangle$ of the broadened peak in TGIC

Table 2. Relative Molar Concentrations of Star Polymer Species in the Aliquots Taken from the Reactor at Various Linking Reaction Times

reaction time (h)	P_1	P_3	P_4	P_5	P_6
0.22	0.701	0.0108	0.0558	0.00647	
0.5	0.698	0.00918	0.0540	0.00852	
8	0.686		0.0380	0.0257	
24	0.638		0.0153	0.0411	0.0128
48	0.616		0.00719	0.0418	0.0241
168	0.575			0.0275	0.0431
336	0.566			0.0138	0.0579
504	0.554			0.00747	0.0643
672	0.545			0.00412	0.0685
840	0.544			0.00198	0.0713

is practically the same as the $\langle M_{LS} \rangle$ of the unlinked arms from the SEC analysis. Therefore the peaks in SEC and TGIC contain species of identical molecular weight, namely, unlinked arms. It seems likely that the single arm species have different end group to which TGIC is sensitive while SEC is not.⁷ All active anions (single arm species) are terminated with methanol (–H as end group) prior to analysis by TGIC and SEC. However, we believe that over the course of the reaction some chains are inadvertently terminated during sampling (which requires removal of small ampules from the reactor with a torch). Although care is taken to rinse away adsorbed polymer (by condensation of solvent in the evacuated polymerization vessel), some termination is apparently occurring over the course of taking numerous samples. The nature of these chain ends is not known, but they appear to strongly affect elution in TGIC.

Although the resolution of TGIC is much better than SEC, it is still not possible to separate the elution peaks of PS₄, PS₅, and PS₆ completely because their molecular weights are too close to each other. Since the peaks are not fully resolved, it is difficult to obtain a precise average molecular weight of each species. Instead, we determined M_{CAL} and M_{LS} at the peak positions of PS₄, PS₅, and PS₆. The results are summarized in the last three columns of Table 1. Unlike the SEC analysis, M_{CAL} and M_{LS} for PS₄, PS₅, or PS₆ provide values closer to the molecular weights expected from the number of arms in each species. As previously reported, M_{CAL} of a branched polymer is much closer to M_{LS} in TGIC than in SEC.⁷

To obtain the relative abundance of each star species, we tried to isolate each peak assuming the Gaussian peak shape as shown in Figure 3, where expanded chromatograms of PS₄, PS₅, and PS₆ are displayed. Fitting to multiple Gaussian peaks was carried out by MicroCal Origin 4.0 software. According to the principle of ideal HPLC separation, an elution peak of a single molecular species is supposed to exhibit a Gaussian peak shape unless it has a strong interaction with stationary phase resulting in peak tailing.²⁹ In this work, however, the PS sample has a narrow but finite molecular weight distribution, and the temperature is varied during the elution. Therefore there is no firm theoretical reason to expect a Gaussian shape of the elution peak. However, empirically a TGIC elution peak of a polymer specimen of narrow molecular weight distribution has a shape very close to Gaussian. For example, the elution peaks of the unlinked arms in the 13 and 30 min chromatograms in Figure 2 can be fit to the Gaussian function very well. We believe that the narrow distribution of the polymer samples and the

small temperature gradient during the elution maintain the separation condition close to the ideal HPLC separation.

In Figure 3, the dotted lines show isolated Gaussian peaks of PS₄, PS₅, or PS₆, and the solid line is the sum of the isolated peaks, which is in good agreement with the chromatogram itself (open circles). From the areas of separated peaks, the fractional abundance of PS₁, PS₂, PS₃, PS₄, PS₅, and PS₆ normalized by the initial concentration of living arms at each linking reaction time can be obtained by eq 1, where P_i is the relative

$$P_i = \frac{A_i / \langle M_{LS} \rangle_i}{\sum_{i=1}^6 A_i / \langle M_{LS} \rangle_{\text{arm}}} \quad \text{and} \quad \sum_{i=1}^6 iP_i = 1 \quad (1)$$

number abundance of PS_{*i*}, subscript *i* denotes the number of arms, and A_i and $\langle M_{LS} \rangle_i$ are the elution peak area and $\langle M_{LS} \rangle$ of PS_{*i*}, respectively. Since the peak area from the UV detection is proportional to the mass concentration, it has to be divided by the molecular weight of the corresponding species to obtain a molar concentration. The thus-obtained time-varying relative abundances of each species are summarized in Table 2 and displayed in Figure 4. In Figure 4, relative amounts of the unlinked arm, P_1 is obtained from both TGIC and SEC chromatograms and plotted with filled (SEC) and open (TGIC) circles. They are in good agreement, confirming that the partially split broad peak in TGIC indeed represents the unlinked arm. The concentration of unlinked arm decreases rapidly at the early stage of the linking reaction, but the reaction rate slows down considerably in the later part of the reaction. This is an expected behavior considering the difficulty of incorporation of the fifth and sixth arms due to steric hindrance. The concentration of PS₄ appears to have reached its maximum already before the first sampling of the reaction mixture and decays as the five-arm and six-arm star polymers are formed. Attachment of the fifth arm is considerably slower than attachment of the previous four arms so that the population of PS₅ is about 12% of PS₄ at the 13 min linking reaction time. PS₅ reaches its maximum abundance after 1–2 days reaction and decays slowly as it is converted to PS₆.

Kinetics of the Linking Reaction. From the time-varying relative abundance of each species with different number of arms, we can extract some quantitative information on the linking reaction rate. Since the initial linking reaction to form PS₂ and PS₃ is much faster than the “synthetic time constant”, i.e., the time required to take an aliquot from the reactor and to terminate the linking reaction, it is impossible to follow the initial linking reaction. As shown in Table 2, after 13 min of reaction a major portion of the linking agent has already formed PS₄, and the concentration of PS₄ has begun to decay. Since there still remains an identifiable amount of PS₃ in the aliquot at the early reaction times, we employed a consecutive reaction model starting from PS₃. In other words, we assumed that PS₃ was formed instantaneously on the time scale of the entire linking reaction. Then the consecutive linking reaction follows the scheme





The linking reaction rates to form PS_4 , PS_5 and PS_6 are as follows.

$$\frac{dP_3}{dt} = -k_4[\text{arm}]P_3 \quad (3)$$

$$\frac{dP_4}{dt} = k_4[\text{arm}]P_3 - k_5[\text{arm}]P_4 \quad (4)$$

$$\frac{dP_5}{dt} = k_5[\text{arm}]P_4 - k_6[\text{arm}]P_5 \quad (5)$$

$$\frac{dP_6}{dt} = k_6[\text{arm}]P_5 \quad (6)$$

The four simultaneous differential equations can be simplified by dividing the other equations by eq 3

$$\frac{dP_4}{dP_3} = -1 + r_5 \frac{P_4}{P_3} \quad (7)$$

$$\frac{dP_5}{dP_3} = -r_5 \frac{P_4}{P_3} + r_6 \frac{P_5}{P_3} \quad (8)$$

$$\frac{dP_6}{dP_3} = -r_6 \frac{P_5}{P_3} \quad (9)$$

where

$$r_5 = \frac{k_5}{k_4} \quad \text{and} \quad r_6 = \frac{k_6}{k_4}$$

The solution of these differential equations are as follows.

$$P_4 = \frac{1}{r_5 - 1}(P_3 - P_3^{r_5}) \quad (10)$$

$$P_5 = \frac{r_5}{(r_5 - 1)(r_6 - 1)}P_3 + \frac{r_5}{(r_5 - r_6)(r_5 - r_6)}P_3^{r_5} - \left[\frac{r_5}{(r_5 - 1)(r_6 - 1)}P_3 + \frac{r_5}{(r_5 - r_6)(r_5 - r_6)} \right]P_3^{r_6} \quad (11)$$

$$P_6 = -\frac{r_5 r_6}{(r_5 - 1)(r_6 - 1)}(P_3 - 1) + \frac{r_6}{(r_5 - r_6)(r_5 - r_6)} \times (P_3^{r_5} - 1) + \left[\frac{r_5}{(r_5 - 1)(r_6 - 1)} + \frac{r_5}{(r_5 - r_6)(r_5 - r_6)} \right] \times (P_3^{r_6} - 1) \quad (12)$$

The linking reaction converting PS_3 into the stars of higher number of arms proceeds so fast that P_3 remains practically nil throughout the observation period. However P_3 can be used as a parameter mediating the relation between P_4 , P_5 , and P_6 as in eqs 10–12. Initial values of r_5 and r_6 were guessed and P_3 was determined by eq 12 for P_6 at various reaction times. Then P_4 and P_5 at the same reaction time were calculated from P_3

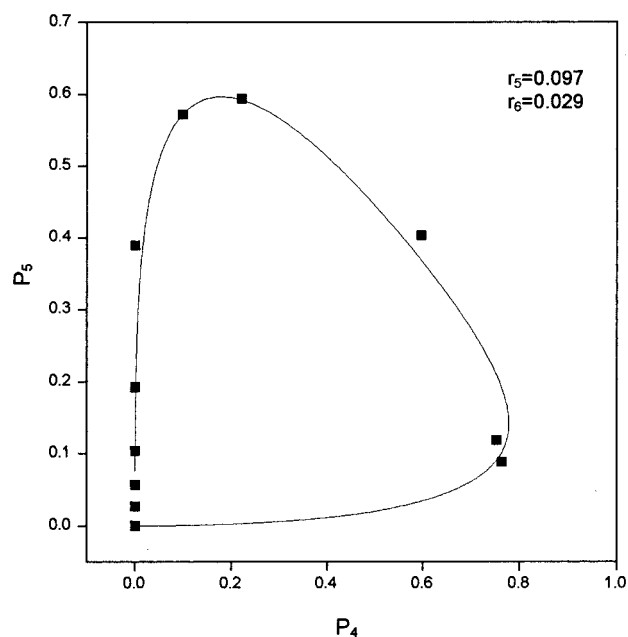


Figure 5. Relation between P_4 and P_5 during the linking reaction. Solid line represents the fit to eqs 10–12.

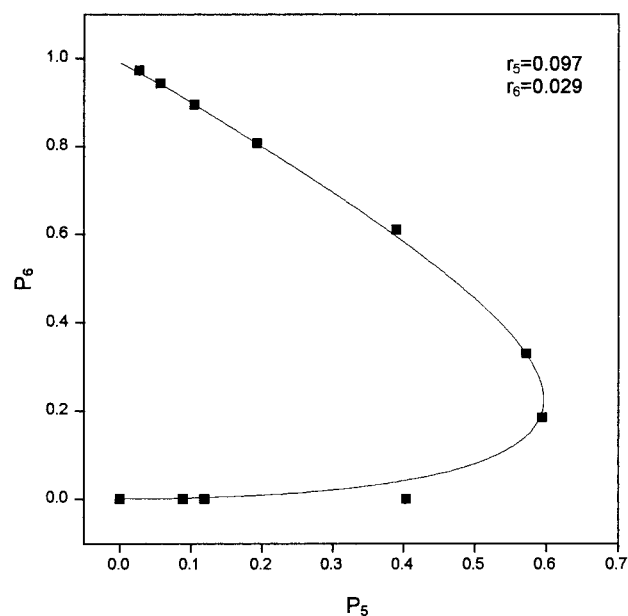


Figure 6. Relation between P_5 and P_6 during the linking reaction. Solid line represents the fit to eqs 10–12.

by eqs 10 and 11. In this way a two parameter optimization process was carried out to obtain the best values of r_5 and r_6 by the least-squares fit of the experimental data of P_4 and P_5 . The best fit result is shown in Figures 5 and 6, where the plots of P_4 vs P_5 and P_5 vs P_6 are shown, respectively. Considering the experimental difficulty associated with the high vacuum technique, as well as the separation to Gaussian peaks, the fitted result appears quite reasonable.

Thus obtained ratios of the rate constants are $r_5 = k_5/k_4 = 0.097$ and $r_6 = k_6/k_4 = 0.029$. Also we can obtain $k_6/k_5 = r_6/r_5 = 0.30$. This result indicates that the linking reaction becomes slower as the number of attached arms increases; the reaction rate of incorporating the fifth arm to PS_4 is 10 times slower than linking the fourth arm to PS_3 while the reaction rate of incorporating the sixth arm to PS_5 is 3 times slower

than attaching the fifth arm to PS₄. The decreasing trend of the reaction rate with the increase of the attached number of arms is as expected; however, it is interesting to note that k_6/k_5 is significantly larger than k_5/k_4 . In fact, this behavior is clearly observed in Figure 4 and Table 2. PS₆ develops rapidly relative to PS₅. When P_5 reaches its maximum, P_6 is already more than 25% of P_5 , while P_5 is only about 10% of P_4 when P_4 reaches its maximum. Although it appears at a glance in contradiction to the expected trend, we believe that the molecular structure of the linking agent and the polymeric anions can provide a clue to explain this observation. The six chlorosilane functional groups do not all reside within a single sphere of steric interaction; instead, they exist as two identical trichlorosilane groups connected by a short spacer, each representing a separate branching point. Considering steric hindrance near the branching points, PS₄ likely has a structure of 2×2 arm star, i.e., two arms are attached to each trichlorosilane group. As far as the steric hindrance in the vicinity of the chlorosilane group is concerned, k_5 and k_6 represent the identical reaction, i.e., linking the anionic end of a living arm polymer to the last chlorosilane group left in a trichlorosilane group while k_4 is the rate constant of incorporating a living arm to one of the two remaining chlorosilane groups. The experimental result appears to reflect this difference of the linking reaction well.

Another consideration is the well-known association of the polymeric anions in benzene. Thus, when one anion reacts with the fifth chlorosilane bond, there is of necessity another anion in close proximity to the sixth chlorosilane group, to facilitate its reaction.

In summary, the kinetics of formation of a model six-arm polystyrene star was studied by TGIC employing light scattering detection. We succeeded in resolving all reaction intermediates and confirmed the conclusion of the previous study of Frater et al.: rapid reaction of the first four arms with the chlorosilane linking agent, slower addition of fifth arm, and even slower addition of the sixth arm. In addition, we were able to extract the quantitative ratio of the linking rate constants, k_5/k_4 and k_6/k_5 . k_5/k_4 was much smaller than k_6/k_5 , which can be explained from the molecular structure of the linking agent.

Acknowledgment. T.C. thanks the Basic Science Research Institute of POSTECH (1RB9712301) and the

Korea Ministry of Education (BSRI-97-3438) for financial support of the research done at POSTECH. J.W.M thanks the Du Pont Company for support of the work done at UAB.

References and Notes

- (1) Zimm, B. H.; Stockmayer, W. H. *J. Chem. Phys.* **1949**, *17*, 130.
- (2) Stockmayer, W. H.; Fixman, M. *Ann. N.Y. Acad. Sci.* **1953**, *57*, 334.
- (3) Zimm, B. H.; Kilb, R. W. *J. Polym. Sci.* **1959**, *37*, 19.
- (4) Small, P. A. *Adv. Polym. Sci.* **1975**, *18*, 1.
- (5) Mays, J. W.; Hadjichristidis, N. *J. Appl. Polym. Sci., Appl. Polym. Symp.* **1992**, *51*, 55.
- (6) Jackson, C.; Frater, D. J.; Mays, J. W. *J. Polym. Sci., Part B: Polym. Phys.* **1995**, *33*, 2159.
- (7) Lee, H. C.; Chang, T.; Harville, S.; Mays, J. W. *Macromolecules* **1998**, *31*, 690.
- (8) Bauer, B. J.; Fetters, L. J. *Rubber Chem. Technol.* **1978**, *51*, 406.
- (9) Roovers, J. In *Encyclopedia of Polymer Science and Engineering*, Kroschwitz, J., Ed.; Wiley: New York, 1989.
- (10) Douglas, J. F.; Roovers, J.; Freed, K. F. *Macromolecules* **1990**, *23*, 4168.
- (11) Roovers, J.; Hadjichristidis, N.; Fetters, L. J. *Macromolecules* **1983**, *16*, 214; Roovers, J.; Zhou, L. L.; Toporowsky, P. M.; van der Zwan, M.; Iatrou, H.; Hadjichristidis, N. *Macromolecules* **1993**, *26*, 4324.
- (12) Pennisi, R. W.; Fetters, L. J. *Macromolecules* **1987**, *20*, 2330.
- (13) Park, I. H.; Choi, E. *Polymer* **1996**, *37*, 313 and references therein.
- (14) Morton, M.; Helminiak, T. E.; Gadkary, S. D.; Bueche, F. *J. Polym. Sci.* **1962**, *57*, 471.
- (15) Frater, D. J.; Mays, J. W.; Jackson, C.; Sioula, S.; Efstradiadis, V.; Hadjichristidis, N. *J. Polym. Sci., Part B: Polym. Phys.* **1997**, *35*, 587 and references therein.
- (16) Storey, R. F.; Kelly, A. S.; Chisholm, B. J. *J. Polym. Sci.: Part A* **1996**, *34*, 2003 and references therein.
- (17) Gervasi, J. A.; Gosnell, A. B. *J. Polym. Sci.: Part A-1* **1966**, *4*, 1391.
- (18) Roovers, J. E. L.; Bywater, S. *Macromolecules* **1972**, *5*, 384.
- (19) Roovers, J. E. L.; Bywater, S. *Macromolecules* **1972**, *7*, 443.
- (20) Lee, H. C.; Chang, T. *Polymer* **1996**, *37*, 5747.
- (21) Lee, H. C.; Lee, W.; Chang, T. *Korea Polym. J.* **1996**, *4*, 160.
- (22) Lee, H. C.; Chang, T. *Macromolecules* **1996**, *29*, 7294.
- (23) Lee, H. C.; Lee, W.; Chang, T. *Makromol. Chem.* **1997**, *118*, 261.
- (24) Lee, W.; Lee, H. C.; Chang, T.; Kim, S. B. *Macromolecules* **1998**, *31*, 344.
- (25) Lee, H. C.; Chang, T. *Bull. Korean Chem. Soc.* **1995**, *16*, 640.
- (26) Lee, H. C.; Chang, T. *Bull. Korean Chem. Soc.* **1996**, *17*, 648.
- (27) Barth, H. G.; Mays, J. W., Eds. *Modern Methods of Polymer Characterization*; John Wiley & Sons: New York, 1991.
- (28) Snyder, L. R.; Kirkland, J. J. *Introduction to Modern Liquid Chromatography*, 2nd ed.; Wiley-Interscience: New York, 1979.

MA971751X